3rd Australian Conference on Industrial Engineering and Operations Management
Sydney, Australia, September 24-26, 2024
Publisher: IEOM Society International, USA DOI: 10.46254/AU03.20240116
Published: September 24, 2024

Reliability Growth Analysis on Centrifugal Slurry Pumps

Rui Zhang, Indra Gunawan and Gopi Chattopadhyay
Maintenance and Reliability Engineering Programmes
Institute of Innovation, Science and Sustainability (IISS)
Federation University Australia
Melbourne, Victoria, Australia
rz2@students.federation.edu.au, indra.gunawan@federation.edu.au,
g.chattopadhyay@federation.edu.au

Zhennian Wang
Superintendent Optimization Project
Operation Optimization Team
Karara Mining Limited (KML)
Perth, Western Australia, Australia
zhennian.wang@kararamining.com.au

Abstract

Centrifugal Slurry Pump (CSP) is one of the most important fluid transportation equipment, widely applied in processing plants. We conduct Reliability Growth Analysis (RGA) on two CSPs, i.e. 352PU342 and 352PU343, in a mineral processing plant at Western Australia (WA), both of which are repairable systems and work in duty-standby mode, to evaluate their maintenance performance during an impeller material transition from metal to rubber. Three Units of Measures (UoMs), i.e. Operating Time (OT), Cumulative Mass (CM), and Effective Work (EW), are employed to accurately quantify the service life of CSPs, the last one of which is constructed by hydraulic modeling and firstly applied in RGA on CSP with embedding the working mechanism, and therefore can better represent the service life. Laplace Test is firstly conducted and reveals the improving performance trends for the CSPs during the impeller transition. Then, two Goodness-of-Fit (GoF) hypothesis tests, i.e. Cramér-von Mises (CVM) Test and Common Beta Hypothesis (CBH) Test, are implemented in sequence to validate that the failure and overhaul data of some of the combinations between impeller and UoM fits Power Law Model, in which the wear-out failure patterns of the CSPs are identified. Finally, economical life models are developed to find out the optimum overhaul interval, i.e. economical life, and the associated minimum average life cost per unit service life for each qualified combination, based on which the overhaul policy simulations of the qualified combinations over an actual operating time frame are compared to figure out the one incurring the lowest total cost, i.e. achieving more than 96.5% cost reduction compared to the current overhaul policy. This study paves the way for massively applying RGA on other critical repairable systems in processing plants, and further lays a solid foundation for Preventative Maintenance Optimisation (PMO), to unlock the hidden substantial value of the existing assets and comply with the relevant Australian Standard (AS).

Keywords
Centrifugal Slurry Pump, Reliability Growth Analysis, Laplace Test and Power Law Model.

1. Introduction

Centrifugal Slurry Pumps (CSPs) are widely used at mineral processing plants for high-flow fluid transportation, the typical wetted parts of which mainly include suction spool, impeller, volute, throat bush, frame liner, and discharge spool (Zhang et al., 2022).

The fluid flows into the impeller domain through the suction spool with total pressure and velocity continuously increasing by impeller propelling and then enters the discharge spool through the volute domain with peak total pressure, vorticity, and velocity around the trailing edges of impeller vanes, which periodically approach and depart from volute tongue area with impeller spinning, resulting in the jet-wake flow structure, the reinforcement effect of the vortexes induced by the trailing edges of impeller vanes and volute tongue area, respectively, and thus high total pressure, vorticity, and wall shear stress around the latter.

Under the two-way interaction between particles and fluid in the granular flow, the trajectories of particles are mostly intersected with the walls of the wetted parts of CSP around the volute tongue and extrados area, which is further confirmed by the erosion analysis in both numerical modeling and field investigation (Zhang et al., 2022).

In a mineral processing plant at Western Australia (WA), two CSPs, i.e. 352PU342 and 352PU343, are configured parallelly in duty-standby mode and serve as pyrite concentrate filter feed pumps, the homogeneous slurry of which comes from the two upstream pyrite concentrate storage tanks, i.e. 352TA022 and 352TA021, respectively, and goes to the downstream pyrite leach distribution box, i.e. 361BX100, together (Figure 1.). Both CSPs are repairable systems with reactive repair and periodical overhaul policies in place, on which Reliability Growth Analysis (RGA) are conducted in the following sections. As per the historical maintenance records, the major failure modes of the CSPs include eroded wetted parts, loose and snap belt, worn pulley groove, failed bearing barrel and motor, in the majority of which the loss energy is dissipated as heat and should be deducted from total power draw when calculating Effective Work (EW) of the CSPs, i.e. the increment of the total mechanical energy of the slurry, including pressure energy, kinetic energy, and gravitational potential energy, energized by the CSPs. Considering that operation parameters and context of CSP, including but not limited to pump speed, flow rate, total dynamic head, available net positive suction pressure, particle density, size, angularity and hardness as well as particle volumetric fraction in the slurry, could have significant impact on the service life of CSP, reliability analysis should be conducted on the data sets under similar operation parameters and context. Both 352PU342 and 352PU343 were upgraded from Warman 3/2 CC-AH to 4/3 CC-AH CSPs in the 2020 CIL uplift project, after which metal and rubber impellers were installed onto the CSPs in sequence to evaluate their performance.

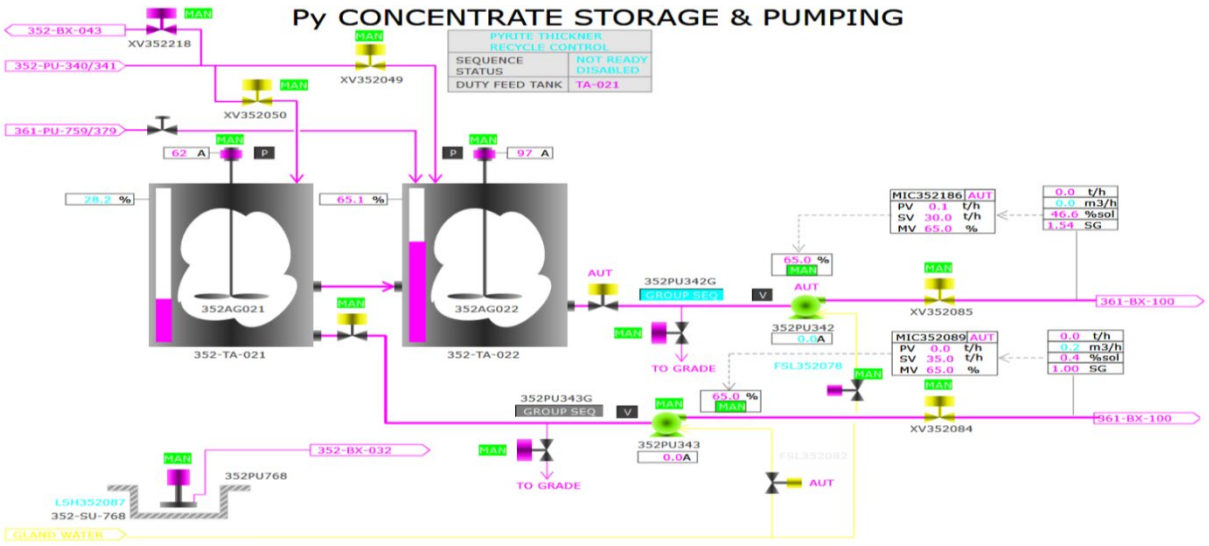

Figure 1. Pyrite concentrates storage and pumping circuit diagram

1.1 Objectives

This study aims to conduct RGA on the service life of the CSPs with employing Laplace Test and Power Law Modeling, to determine the optimal Units of Measure (UoMs), impeller material and overhaul policy combination.

2. Units of Measure Selection

To accurately measure the service life of the CSPs under their major failure modes, Operating Time (OT), Cumulative Mass (CM), and EW are employed as three UoMs, the last one of which is firstly applied in RGA on CSP with the working mechanism informed, and therefore has better performance on the service life measurement than the other UoMs. EW is calculated in

$$EW = \int_{t_s}^{t_e} EP\, dt. \tag{1}$$

Where t_s and t_e are the start and end time, respectively, and EP is the effective power of the CSP. EP is calculated in

$$EP = ER_o - ER_i. \tag{2}$$

Where ER_o and ER_i are the slurry energy rates at the outlet and inlet port of the CSP, respectively. ER_i is calculated in

$$ER_i = \frac{1}{2}\rho v_i^2 \cdot \Delta V + \rho g h_t \cdot \Delta V. \tag{3}$$

Where ρ is the density of the slurry, v_i is the inlet velocity of the CSP, ΔV is the slurry volumetric flow rate of the CSP, g is the gravitational acceleration, set as 9.81 ($m \cdot s^{-2}$) in this study, and h_t is the Relative Level (RL) of the slurry surface of 352TA022 or 352TA021 (McDonough, 2009).

ER_o is calculated in

$$ER_o = ER_e + EL_d. \tag{4}$$

Where ER_e is the slurry energy rate at the end of the discharge pipe of the CSP, i.e. the inlet port of 361BX100, which is assumed to be at 1 atmospheric pressure due to the installed ventilation tube, and EL_d is the energy loss rate along the discharge pipe of the CSP to the inlet port of 361BX100. ER_e is calculated in

$$ER_e = \frac{1}{2}\rho v_e^2 \cdot \Delta V + \rho g h_b \cdot \Delta V. \tag{5}$$

Where v_e is the inlet velocity of 361BX100 from the CSP, and h_b is the RL of the top surface of 361BX100 inlet port connected to the discharge pipe of the CSP, set as 5511.7 (m) (McDonough, 2009).

EL_d is calculated in

$$EL_d = EL_d^{major} + EL_d^{minor}. \quad (6)$$

Where EL_d^{major} and EL_d^{minor} are the major or friction energy loss rate of the main straight pipe sections and minor or dynamic energy loss rate of the main pipe fittings along the discharge pipe of the CSP to the inlet port of 361BX100, respectively. Based on the Darcy-Weisbach equation (Cengel and Cimbala, 2019), EL_d^{major} is calculated in

$$EL_d^{major} = \frac{1}{2}\rho f_d \frac{L_d}{D_d} v_d^2 \cdot \Delta V. \quad (7)$$

Where f_d, L_d, D_d, and v_d are the friction factor, length, hydraulic diameter, and velocity of the discharge pipe of the CSP to the inlet port of 361BX100, respectively. f_d is calculated in

$$\frac{1}{\sqrt{f_d}} = -1.8log\left[\frac{6.9}{Re_d} + \left(\frac{\varepsilon_d/D_d}{3.7}\right)^{1.11}\right]. \quad (8)$$

Where Re_d and ε_d are the Reynolds number and internal surface roughness of the discharge pipe of the CSP to the inlet port of 361BX100, respectively. In this study, $\varepsilon_d = 0.0000015\ (m)$ is adopted for the HDPE discharge pipe. Re_d is calculated in

$$Re_d = \frac{\rho v_d D_d}{\mu}. \quad (9)$$

Where μ is the dynamic viscosity of the slurry, and in this study, $\mu = 0.06\ (N \cdot s \cdot m^{-2})$ is adopted for the pyrite concentrate.

EL_d^{minor} is calculated in

$$EL_d^{minor} = \frac{1}{2}\rho K_L v_d^2 \cdot \Delta V. \quad (10)$$

Where K_L is the local loss coefficient of the main pipe fittings along the discharge pipe of the CSP to the inlet port of 361BX100 (Cengel and Cimbala, 2019).

3. Laplace Test

Considering that Life Data Analysis (LDA) is applicable on non-repairable system, while RGA is more suitable on repairable system (Crow, 2003), RGA are conducted on both repairable CSPs with employing Laplace Test and Power Law Modeling, which is an extension of Weibull distribution modeling, in this study (Figure 2) (AS/NZS IEC 61649, 2020) (AS IEC 61164, 2018) (AS/NZS IEC 61703, 2020).

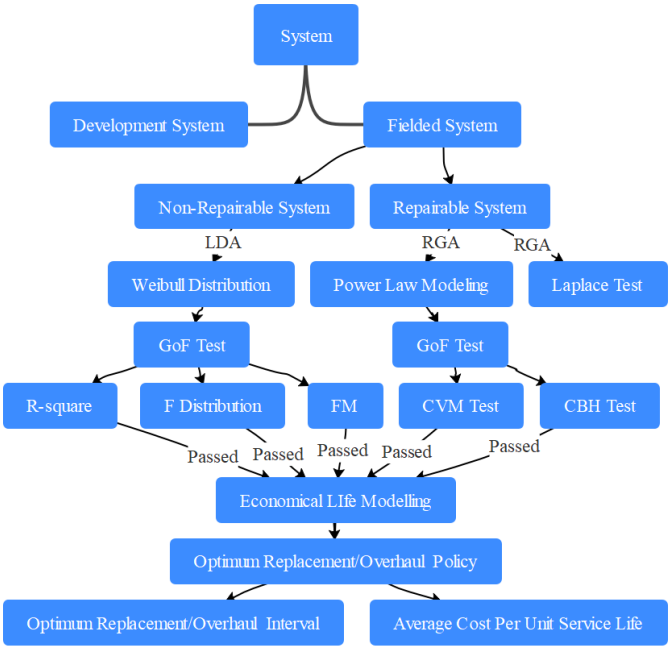

Figure 2. Reliability analysis flow chart

To analyze the impact of changing the material of the impeller from metal to rubber on the trends of the failure rates of the CSPs, Laplace Test is conducted to evaluate its null hypothesis, H_L, that there is no trend during the designated period. The test statistic in Laplace Test, U, which would approximately follow the standard normal distribution if H_L is true, is constructed in

$$U = \frac{\frac{\sum_{i=1}^{N_L} X_{Li}}{N_L} - \frac{T_L}{2}}{T_L\sqrt{\frac{1}{12N_L}}}. \quad (11)$$

Where X_{Li}, T_L, and N_L are the service life of the i^{th} successive maintenance event, total service life, and total number of maintenance events in the Laplace Test, respectively (Crow, 2003).

To exclude the impact of other impact factors on the trends, Laplace Test is firstly conducted on 352PU343 with metal or rubber impeller applied only. Table 1. indicates that all three UoMs of 352PU343 with a metal or rubber impeller applied only fail to reject H_L at a significance level of 0.1, a widely applied threshold for Laplace Test in the industry. Considering that 352PU342 and 352PU343 work in similar working scenarios with the same components and configurations applied, it can be concluded that there are no trends in the failure rates of the CSPs with metal or rubber impeller applied only at the 0.1 significance level.

Table 1. Laplace Test on 352PU343 with rubber or metal impeller

Impeller	**Metal**			**Rubber**		
UoM	OT	CM	EW	OT	CM	EW
N_L	8			5		
T_L	834 (h)	77741 (t)	1036 (kw.h)	1178 (h)	100907 (t)	1217 (kw.h)
X_{L1}	92 (h)	8070 (t)	104 (kw.h)	57 (h)	4590 (t)	54 (kw.h)
X_{L2}	192 (h)	15902 (t)	229 (kw.h)	138 (h)	11462 (t)	119 (kw.h)
X_{L3}	236 (h)	20039 (t)	319 (kw.h)	157 (h)	12944 (t)	137 (kw.h)
X_{L4}	253 (h)	21374 (t)	373 (kw.h)	651 (h)	55132 (t)	647 (kw.h)
X_{L5}	314 (h)	27180 (t)	436 (kw.h)	885 (h)	76817 (t)	923 (kw.h)
X_{L6}	474 (h)	42970 (t)	637 (kw.h)			
X_{L7}	607 (h)	56485 (t)	778 (kw.h)			
X_{L8}	665 (h)	61416 (t)	858 (kw.h)			
U	-0.740	-0.906	-0.486	-1.391	-1.402	-1.480
P_L	0.459	0.365	0.627	0.164	0.161	0.139

Where P_L is the lowest significance level to reject H_L.

Then, Laplace Test is conducted on both CSPs during the transition from metal to rubber impeller, respectively. Table 2. shows that all three UoMs of 352PU342 during the transition fail to reject H_L at the 0.1 significance level, while for 352PU343 during the transition, OT and CM reject H_L at the 0.1 significance level and EW rejects H_L at a significance level of 0.105, slightly higher than 0.1.

Table 2. Laplace Test on both CSPs during the transition from metal to rubber impeller

CSP	**352PU342**			**352PU343**		
UoM	OT	CM	EW	OT	CM	EW
N_L	4			14		
T_L	2465 (h)	251744 (t)	3969 (kw.h)	2013 (h)	178647 (t)	2253 (kw.h)
X_{L1}	1171 (h)	92016 (t)	1316 (kw.h)	92 (h)	8070 (t)	104 (kw.h)
X_{L2}	1612 (h)	168601 (t)	2941 (kw.h)	192 (h)	15902 (t)	229 (kw.h)
X_{L3}	2015 (h)	211162 (t)	3443 (kw.h)	236 (h)	20039 (t)	319 (kw.h)
X_{L4}	2251 (h)	233470 (t)	3712 (kw.h)	253 (h)	21374 (t)	373 (kw.h)
X_{L5}				314 (h)	27180 (t)	436 (kw.h)
X_{L6}				474 (h)	42970 (t)	637 (kw.h)
X_{L7}				607 (h)	56485 (t)	778 (kw.h)
X_{L8}				665 (h)	61416 (t)	858 (kw.h)
X_{L9}				834 (h)	77741 (t)	1036 (kw.h)
X_{L10}				892 (h)	82331 (t)	1090 (kw.h)
X_{L11}				973 (h)	89203 (t)	1155 (kw.h)
X_{L12}				991 (h)	90684 (t)	1173 (kw.h)
X_{L13}				1485 (h)	132873 (t)	1683 (kw.h)
X_{L14}				1719 (h)	154558 (t)	1959 (kw.h)
U	1.489	1.388	1.516	-2.007	-1.916	-1.620
P_L	0.137	0.165	0.129	0.045	0.055	0.105

To clarify the contradiction of the results of the Laplace Test conducted on the CSPs during the transition, a sensitivity test is further conducted to figure out the relationship between P_L and N_L. Figure 3. illustrates that with the increasing of N_L, the plots of P_L for all three UoMs show overall decreasing trends with a few fluctuations in the middle, and finally become stable below 0.11 when $N_L \geq 12$. In this case, the result of the Laplace Test conducted on 352PU343 during the transition with $N_L = 14$ is accepted, rather than that on 352PU342 with $N_L = 4$. Thus, it can be concluded that there are decreasing trends of the failure rates of 352PU342 and 352PU343 during the transition from metal to rubber impeller, i.e. the performance of the CSPs is improving during the transition due to the application of rubber impeller instead of the metal one, at the 0.105 significance level.

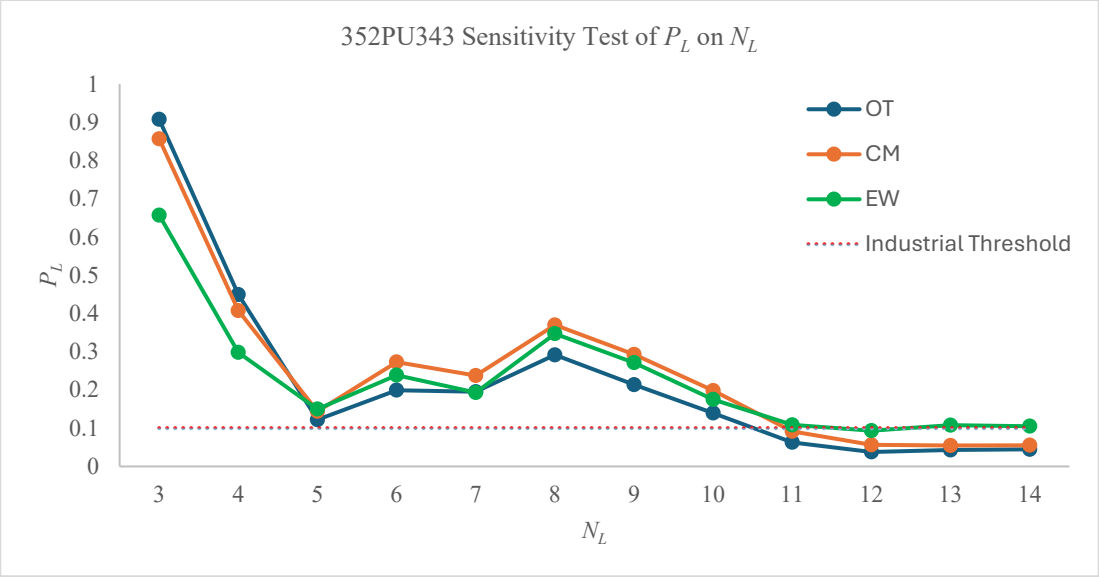

Figure 3. 352PU343 Sensitivity test of $\boldsymbol{P_L}$ on $\boldsymbol{N_L}$

4. Cramér-von Mises Test

Before conducting Power Law Modeling, a few Goodness-of-Fit (GoF) hypothesis tests are conducted to validate that the failure data fit Power Law Model, the 1st one of which is Cramér-von Mises (CVM) Test with its null hypothesis, H_{CVM}, that the failure data follow a Non-Homogeneous Poisson Process (NHPP) with the failure intensity function

$$u(t) = \lambda\beta t^{\beta-1}. \tag{12}$$

Where $u(t)$ is the failure intensity of Power Law Model, λ and β are the two parameters of Power Law Model, and t is the service life (AS/NZS IEC 61710, 2020).

The test statistic in CVM Test, C_M^2, is calculated in

$$C_M^2 = \frac{1}{12M} + \sum_{j=1}^{M}\left(Z_j^{\bar{\beta}} - \frac{2j-1}{2M}\right)^2. \tag{13}$$

Where M is the total failure number in all the systems, Z_j is the j^{th} element in a data set of positive real numbers, $\{Z_1, Z_2, \dots, Z_M\}$, each element of which is not larger than 1 and one-to-one mapping to the element, Y_{iq}, by sorting the data set formed by the latter in an ascending order, and $\bar{\beta}$ is the unbiased Maximum Likelihood Estimation (MLE) of β (AS/NZS IEC 61710, 2020) (Crow, 1990). M is calculated in

$$M = \sum_{q=1}^{K} M_q. \tag{14}$$

Where K is the number of the repairable systems and M_q is the failure number in the q^{th} repairable system.

Y_{iq} is calculated in

$$Y_{iq} = \frac{X_{iq}}{T_q}, i = 1, 2, \dots, M_q, q = 1,2, \dots, K. \tag{15}$$

Where X_{iq} and T_q are the service life of the i^{th} failure and total service life in the q^{th} repairable system.

$\bar{\beta}$ is calculated in

$$\bar{\beta} = \frac{M-1}{\sum_{q=1}^{K}\sum_{i=1}^{Mq} ln\left(\frac{1}{Y_{iq}}\right)}. \quad (16)$$

Table 3, 4, 5, 6, 7, and 8. illustrate the raw input data for CVM Test on all the three UoMs of the CSPs with metal and rubber impeller, respectively, the results of which are shown in Table Ⅸ. It can be concluded that five of six combinations between UoM and impeller fail to reject H_{CVM} and thus pass CVM Test at a significance level of 0.2, the most stringent threshold for CVM Test, while the combination between OT and rubber impeller rejects H_{CVM} and thus fails to pass CVM Test at any significance level.

Table 3. Raw input data for CVM Test on ***OT*** of the CSPs with metal impeller

CSP	352PU342		352PU343			
System	1	2	3	4	5	6
T_q (h)	1611.58	403.39	44.65	16.66	412.13	169.16
X_{1q} (h)	1170.57				60.92	
X_{2q} (h)					221.63	
X_{3q} (h)					354.25	

Table 4. Raw input data for CVM Test on ***CM*** of the CSPs with metal impeller

CSP	352PU342		352PU343			
System	1	2	3	4	5	6
T_q (t)	168601.33	42560.68	4137.64	1334.43	40042.27	16324.56
X_{1q} (t)	92015.78				5806.26	
X_{2q} (t)					21596.45	
X_{3q} (t)					35110.66	

Table 5. Raw input data for CVM Test on ***EW*** of the CSPs with metal impeller

CSP	352PU342		352PU343			
System	1	2	3	4	5	6
T_q (kw.h)	168601.33	42560.68	4137.64	1334.43	40042.27	16324.56
X_{1q} (kw.h)	92015.78				5806.26	
X_{2q} (kw.h)					21596.45	
X_{3q} (kw.h)					35110.66	

Table 6. Raw input data for CVM Test on ***OT*** of the CSPs with rubber impeller

CSP	352PU342		352PU343			
System	1	2	3	4	5	6
T_q (h)	235.62	879.09	156.67	494.02	527.70	6.14
X_{1q} (h)		214.04	57.49		233.95	
X_{2q} (h)		736.31	138.46			

Table 7. Raw input data for CVM Test on $\boldsymbol{CM}$ of the CSPs with rubber impeller

CSP	352PU342		352PU343			
System	1	2	3	4	5	6
T_q (t)	22308.27	53196.56	12943.73	42188.21	45774.73	1035.78
X_{1q} (t)		18273.85	4589.84		21685.39	
X_{2q} (t)			11461.89			

Table 8. Raw input data for CVM Test on $\boldsymbol{EW}$ of the CSPs with rubber impeller

CSP	352PU342		352PU343			
System	1	2	3	4	5	6
T_q (kw.h)	268.44	831.49	136.80	510.37	569.87	21.17
X_{1q} (kw.h)		257.07	53.60		275.73	
X_{2q} (kw.h)			119.19			

Table 9. CVM Test results on all the three UoMs of the CSPs with both metal and rubber impeller

Impeller	Metal			Rubber		
UoM	OT	CM	EW	OT	CM	EW
C_M^2	0.059	0.063	0.045	0.554	0.092	0.075
α_{CVM}	0.20	0.20	0.20	N/A	0.20	0.20

Where α_{CVM} is the highest significance level to fail to reject H_{CVM}.

5. Common Beta Hypothesis Test

The 2nd GoF hypothesis test for the validation of the failure data against Power Law Model is Common Beta Hypothesis (CBH) Test with its null hypothesis, H_{CBH}, that all the systems to be applied in Power Law Model have

similar values of β. The test statistic in CBH Test, D, which would approximately follow the Chi-squared distribution with $(K-1)$ Degrees of Freedom (DoF) if H_{CBH} is true, is constructed in

$$D = \frac{2L}{a}. \tag{17}$$

Where L and a are the two statistics in CBH Test (AS/NZS IEC 61710, 2020) (Ascher and Feingold, 1984). L is calculated in

$$L = \sum_{q=1}^{K} M_q ln\,(\tilde{\beta}_q) - Mln(\beta^*). \tag{18}$$

Where $\tilde{\beta}_q$ denotes the conditional MLE of β_q, shape factor in the Power Law Model in the q^{th} repairable system, and β^* is a function of $\tilde{\beta}_q$ (Erto and Lepore, 2017). $\tilde{\beta}_q$ is calculated in

$$\tilde{\beta}_q = \frac{M_q}{\sum_{i=1}^{M_q} ln\,(\frac{1}{Y_{iq}})}. \tag{19}$$

β^* is calculated in

$$\beta^* = \frac{M}{\sum_{q=1}^{K} \frac{M_q}{\tilde{\beta}_q}}. \tag{20}$$

a is calculated in

$$a = 1 + \frac{1}{6(K-1)}\left[\sum_{q=1}^{K} \frac{1}{M_q} - \frac{1}{M}\right]. \tag{21}$$

Table 10. indicates that all the five combinations between UoM and impeller fail to reject H_{CBH} and thus pass CBH Test at a significance level of 0.1, a widely applied threshold for CBH Test in the industry.

Table 10. CBH Test results on the UoMs of the CSPs with both metal and rubber impeller

Impeller	Metal			Rubber	
UoM	*OT*	*CM*	*EW*	*CM*	*EW*
System	1, 5			2, 3, 5	
D	0.556	0.090	0.016	0.222	0.366
P_{CBH}	0.912	0.471	0.201	0.210	0.334

Where P_{CBH} is the highest significance level to fail to reject H_{CBH}.

6. Power Law Model

Power Law Modeling is conducted on the above five combinations between UoM and impeller, which pass both CVM Test and CBH Test. $\hat{\beta}$ and $\hat{\lambda}$ denote the general MLE of β and λ, respectively (AS/NZS IEC 61710, 2020) (Crow, 1990). $\hat{\beta}$ is calculated in

$$\hat{\beta} = \frac{M}{\hat{\lambda}\sum_{q=1}^{K}\left[T_q^{\hat{\beta}} Ln(T_q)\right] - \sum_{q=1}^{K}\sum_{i=1}^{Mq} Ln(X_{iq})}. \tag{22}$$

$\hat{\lambda}$ is calculated in

$$\hat{\lambda} = \frac{M}{\sum_{q=1}^{K} T_q^{\hat{\beta}}}. \tag{23}$$

β_L and β_U denote the Crow two-sided lower and upper Confidence Bounds (CBs) on β, respectively. β_L is calculated in

$$\beta_L = \hat{\beta}\frac{\chi^2_{\frac{\alpha_{PL}}{2},2M}}{2M}. \tag{24}$$

Where $\chi^2_{\frac{\alpha_{PL}}{2},2M}$ is the value of a random variable, which follows the Chi-squared distribution with $2M$ DoF, with Cumulative Distribution Function (CDF) equaling to $\frac{\alpha_{PL}}{2}$, and α_{PL} is the significance level of CBs on both β and λ, set as 0.1, a widely applied threshold for Power Law Model in the industry, in this study (AS/NZS IEC 61710, 2020) (Crow, 1993).

β_U is calculated in

$$\beta_U = \hat{\beta}\frac{\chi^2_{1-\frac{\alpha_{PL}}{2},2M}}{2M}. \tag{25}$$

Where $\chi^2_{1-\frac{\alpha_{PL}}{2},2M}$ is the value of a random variable, which follows the Chi-squared distribution with $2M$ DoF, with CDF equaling to $\left(1-\frac{\alpha_{PL}}{2}\right)$ (AS/NZS IEC 61710, 2020) (Crow, 1993).

Similarly, λ_L and λ_U denote the Crow two-sided lower and upper Confidence Bounds (CBs) on λ, respectively. λ_L is calculated in

$$\lambda_L = \frac{\chi^2_{\frac{\alpha_{PL}}{2},2M}}{2\cdot\sum_{q=1}^{K} T_q^{\hat{\beta}}}. \tag{26}$$

λ_U is calculated in

$$\lambda_U = \frac{\chi^2_{1-\frac{\alpha_{PL}}{2},2M+2}}{2\cdot\sum_{q=1}^{K} T_q^{\hat{\beta}}}. \tag{27}$$

Considering that in this study, the sample sizes of all the five combinations are small (Gunawan, 2023), i.e. $M < 30$, the initial value of $\hat{\beta}$ is calculated firstly, following by which the initial value of β_U is derived and then treated as the adjusted value of $\hat{\beta}$ for the further calculation on the adjusted values of $\hat{\lambda}$ and the corresponding CBs (Crow, 1993). Table 11. indicates the adjusted values of $\hat{\beta}$ and $\hat{\lambda}$ in the five combinations, which are all inside their CBs, respectively.

Table 11. Adjusted Power Law parameters and the CBs of the combinations between impeller and UoM

Impeller	Metal			Rubber	
UoM	OT	CM	EW	CM	EW
System	1, 5			2, 3, 5	
$\hat{\beta}$	1.38	1.29	1.09	1.58	1.42
β_L	0.47	0.44	0.37	0.54	0.49
β_U	2.68	2.50	2.11	3.07	2.76
$\hat{\lambda}$	1.26E-04	6.14E-07	5.90E-04	6.99E-08	1.68E-04
λ_L	4.30E-05	2.10E-07	2.02E-04	2.39E-08	5.75E-05
λ_U	2.88E-04	1.41E-06	1.35E-03	1.60E-07	3.85E-04

7. Economical Life Model

Considering that $\hat{\beta}$ in the five combinations in Table 11. are all larger than 1, indicating the wear-out failure pattern, it is recommended to establish an overhaul policy on both 352PU342 and 352PU343 to achieve minimum average life cost per unit service life, denoted as CR_O, by setting up optimum overhaul interval, i.e. economical life, denoted as T_O (Crow, 2012) (Zhang et al., 2017), which is calculated in

$$T_O = \left[\frac{\bar{O}}{\lambda(\beta-1)\bar{R}}\right]^{1/\beta}. \tag{28}$$

Where $\bar{R}$ and $\bar{O}$ denote the average cost of repair and overhaul, respectively.

CR_O is calculated in

$$CR_O = \frac{\bar{O}+\bar{R}\lambda T_O^{\beta}}{T_O}. \tag{29}$$

Table 12. indicates the estimated values of the main parameters in the economical life models of the five combinations.

Table 12. Economical life model parameters of the combinations between impeller and UoM

Impeller	Metal			Rubber	
UoM	OT	CM	EW	CM	EW
System	1, 5			2, 3, 5	
$\bar{R}$ (\$)	375.20			1114.46	
$\bar{O}$ (\$)	8261.95			6923.40	
$\hat{T}_O$	1.22E+04 (h)	1.84E+06 (t)	1.49E+05 (kw.h)	1.48E+05 (t)	2.96E+03 (kw.h)
$\widehat{CR}_O$	7.43E-01 (\$/h)	4.80E-03 (\$/t)	2.97E-01 (\$/(kw.h))	4.69E-02 (\$/t)	2.61E+00 (\$/(kw.h))

Where $\hat{T}_O$ and $\widehat{CR}_O$ denote the general MLE of T_O and CR_O, respectively.

8. Overhaul Policy Simulations in The Actual Working Scenario

To figure out the best overhaul policy from the cost reduction perspective, the five combinations between impeller and UoM under T_O are simulated during 22/12/2022 ~ 20/11/2023 for 352PU342 and 13/09/2022 ~ 30/12/2023 for 352PU343, the total costs of which are normalized and compared to the actual one under the existing eight-calendar-weeks overhaul policy with using both metal and rubber impeller. Table 13. shows that when using the same impeller under T_O, the total cost of EW is lower than that of CM, which is also lower than that of OT, and when using the same UoM under T_O, the total cost of metal impeller is much lower than that of rubber one. Moreover, the combination between the metal impeller and EW under T_O achieves the best cost reduction performance, i.e. a reduction of more than 96.5% in the total cost compared to the actual one, among the five combinations.

Table 13. Cost comparison of the overhaul policy simulations in the actual working scenario

Impeller	Metal and Rubber	Metal			Rubber	
UoM	CT	OT	CM	EW	CM	EW
Cumulative Service Life	1.93E+04 (h)	4.67E+03 (h)	4.50E+05 (t)	6.59E+03 (kw.h)	4.50E+05 (t)	6.59E+03 (kw.h)
Normalized Total Cost	100.00%	5.95%	3.71%	3.35%	36.25%	29.45%

Where CT denotes the calendar time, which is employed as the UoM in the existing overhaul policy.

9. Conclusion

In this study, we conducted RGA on two CSPs in a mineral processing plant at WA, i.e. 352PU342 and 352PU343, which experienced a transition from metal to rubber impeller, by employing Laplace Test and Power Law Model. To accurately measure the service life and evaluate the performance of the CSPs, three UoMs, i.e. OT, CM, and EW, were constructed and employed, the last one of which is firstly applied in RGA on CSP with the working mechanism informed, and thus can better measure the service life.

Laplace Test indicated the decreasing trends of the failure rates of the CSPs during the impeller material transition at the 0.105 significance level. Two GoF hypothesis tests, i.e. CVM Test and CBH Test, validated that the failure and overhaul data of the five of six combinations between UoM and impeller fitted Power Law Model, which furtherly revealed the wear-out failure patterns of the CSPs, at the significance level of 0.2 and 0.1, respectively.
Based on the adjusted Power Law parameters, economical life models were established to determine T_O and CR_O in the selected combinations, the overhaul policies based on which were simulated in the actual working scenario to identify the one offering the best cost optimization. Finally, it is recommended to implement the CSPs overhaul policy in the interval of 1.49E+05 (kw.h) by using the metal impeller and EW to minimize the total cost, i.e. achieving over 96.5% cost reduction compared to the existing eight-calendar-weeks overhaul policy with using both metal and rubber impeller.

This study successfully validated the feasibility of conducting RGA based on the high-quality field data, and moreover can serve as a standard procedure and technical guide to widely conduct RGA on other critical repairable systems, such as conveyor belt, in processing plants for substantial cost reduction, which will not only revolutionise the existing Preventive Maintenance (PM) strategies and tactics on repairable systems in the processing plant, to furtherly lay a solid foundation for Preventive Maintenance Optimisation (PMO), but also work as one of two cornerstones or pillars in the best industrial practices in reliability engineering and asset health or management sector, including but not limited to Reliability Block Diagram (RBD), Fault Tree Analysis (FTA), Markov State Space (MSS) and Monte Carlo Simulation (MCS), and more importantly comply with the latest Australian Standard (AS) and International Standard (IS), i.e. AS/NZS IEC 61710:2020 and IEC 61710:2013, to furtherly unlock the hidden value of the existing assets. Future research should involve more data sets with larger scales and employ more localized UoMs strongly correlated to the most dominant failure modes, such as energy dissipation, the integral of thermal and vibration signals over time, to further improve the accuracy of RGA and thus reduce the total cost to the maximum extent. Moreover, detailed cost-benefit analysis and Life Cycle Cost (LCC) modeling should be conducted to further optimise the maintenance strategies of the CSPs.

Acknowledgment

The authors thank the site reliability engineering and metallurgy team for the great support and inspiration.

References

Zhang, R., Gou, D. Z. and Yang, R. Y., Numerical Modeling of Wall Erosion in Centrifugal Slurry Pumps, *Proceedings of the 2nd Int. Conf. Mineral Engineering and Materials Science*, Sydney, Australia, Nov. 27-30, 2022.

McDonough, J. M., *Lectures In Elementary Fluid Dynamics: Physics, Mathematics and Applications*, Lexington, KY, USA: University of Kentucky, Lexington, pp. 1-164, 2009.

Cengel, Y. A. and Cimbala, J. M., *Fluid Mechanics*, 4th ed., McGraw Hill, 2019.

Crow, L. H., Methods for Reducing the Cost to Maintain a Fleet of Repairable Systems, *Annual Reliability and Maintainability Symposium*, Tampa, USA, Jan. 27-30, pp. 392-399, 2003.
Joint Technical Committee QR-005, Dependability., Weibull analysis, *AS/NZS IEC 61649*, May 2020.
Technical Committee QR-005, Dependability., Reliability growth-Statistical test and estimation methods, *AS IEC 61164*, Jul. 2018.
Joint Technical Committee QR-005, Dependability., Mathematical expressions for reliability, availability, maintainability and maintenance support terms, *AS/NZS IEC 61703*, May 2020.
Joint Technical Committee QR-005, Dependability., Power law model - Goodness-of-fit tests and estimation methods, *AS/NZS IEC 61710*, Apr. 2020.
Crow, L. H., Evaluating the Reliability of Repairable Systems, *Annual Reliability and Maintainability Symposium*, Los Angeles, USA, Jan. 23-25, pp. 275-279, 1990.
Ascher, H. and Feingold, H., *Repairable Systems Reliability*, CRC Press/Marcel Dekker, Inc., 1984.
Erto, P. and Lepore, A., Reliability of Repairable Valves: Analysis of Failure Times from Chemical Plants, *International Journal of Engineering Research and Applications*, vol. 7, no. 8, pp. 19-24, Jul. 2017.
Crow, L. H., Confidence Intervals on the Reliability of Repairable Systems, *Annual Reliability and Maintainability Symposium*, Atlanta, USA, Jan. 26-28, pp. 126-134, 1993.
Gunawan, I., *Course Book: MREGC5101 Basic Quantitative Skills for Reliability Engineering*, Melbourne, VIC, AU: Federation University Australia, pp. 67-68, 2023.
Crow, L. H., Demonstrating reliability growth requirements with confidence, *Annual Reliability and Maintainability Symposium*, Reno, USA, Jan. 23-26, pp. 1-6, 2012.
Zhang, J. L., Sun, F. B. and Sarakakis, G., Field reliability growth modeling for automotive, *Annual Reliability and Maintainability Symposium*, Orlando, USA, Jan. 23-26, pp. 1-7, 2017.

Biographies

Rui Zhang is currently a last-year student in Master of Maintenance and Reliability Engineering Program within the Institute of Innovation, Science and Sustainability (IISS), at Federation University Australia. He has over six years' working experience in the maintenance and reliability engineering sector in the mining industry.

Zhennian Wang is currently a Superintendent Optimization Project within the Operation Optimization Team, at Karara Mining Limited (KML). He has over twenty-five years' working experience in the maintenance and reliability engineering sector in the mining industry.

Indra Gunawan is currently an Associate Professor in Complex Project Management and Program Coordinator of Postgraduate Project Management in the Adelaide Business School, Faculty of Arts, Business, Law and Economics, at the University of Adelaide, South Australia. Previously, he worked in the School of Engineering and Information Technology at Monash University, Gippsland Campus as a Coordinator for Maintenance and Reliability Engineering Programs. He has also served as a faculty in the Department of Mechanical and Manufacturing Engineering at Auckland University of Technology, New Zealand and the Head of Systems Engineering and Management program at Malaysia University of Science and Technology.

Gopi Chattopadhyay is currently a Post Graduate Program Coordinator of Maintenance and Reliability Engineering within the Institute of Innovation, Science and Sustainability (IISS), at Federation University Australia. He has over 40 years' experience in the industry and university in the area of Asset Management, Maintenance, Reliability, Operations, Project Planning, Quality, Cost Engineering and Engineering Management.